Three-dimensional analysis of the dopant potential of a silicon *p-n* junction by holographic tomography

A C Twitchett, T J V Yates, P K Somodi, S B Newcomb[1], R E Dunin-Borkowski and P A Midgley

Department of Materials Science and Metallurgy, University of Cambridge, Pembroke Street, Cambridge, CB2 3QZ, UK
[1] Sonsam Ltd., Glebe Laboratories, Newport, Co. Tipperary, Ireland

ABSTRACT: Off-axis electron holography and tomography have been combined to examine the 3-D electrostatic potential associated with a Si *p-n* junction. The device was prepared in a novel specimen geometry using focused ion beam milling and a series of holograms was acquired over a tilt range of -70º to +70º. Simultaneous iterative reconstruction was used to reconstruct the 3-D electrostatic potential in the specimen. The experimental results were compared to simulations of the potential variation. Quantitative results from the central, 'bulk' semiconducting regions and from the surface layers were extracted from the 3-D reconstruction.

1. INTRODUCTION

Dopant profiling of semiconductor devices using off-axis electron holography has become more widely used in recent years, with many examples of the successful visualisation of dopant-related electrostatic potentials (e.g. McCartney et al 2002; Twitchett et al 2005). Although electron holography promises to provide fully quantitative results, the measured potential is a 2-D projection along the electron beam direction through the semiconductor membrane thickness, including all surface potential effects. These surface contributions are particularly significant when using electron holography to examine semiconductor device structures prepared from site-specific regions of device structures using focused ion beam (FIB) milling. This preparation technique is known to generate amorphous and electrically altered near-surface layers. In order to obtain a quantitative characterisation of the bulk and surface properties of a semiconductor membrane, a 3-D map of the electrostatic potential variation is required.

Electron tomography has been applied successfully to a number of different problems in materials science, in particular to the examination of catalysts and other small inorganic particles (Midgley and Weyland 2003). This technique involves the use of a series of images acquired over a large range of tilt angles to reconstruct 3-D properties of a specimen. However, its application in the fields of semiconductors and electron holography has been limited to date. The phase signal reconstructed from off-axis electron holograms satisfies the tomographic requirement that the signal is a monotonic function of the sample thickness, and it should therefore be possible to reconstruct the 3-D phase (and, therefore, the related electrostatic potential) associated with a doped semiconductor device. This measurement is particularly important for the quantitative determination of the electrostatic potential at an FIB-modified semiconductor surface, but also has significant relevance to the examination of many nanoscale semiconductor structures.

2. EXPERIMENTAL DETAILS

2.1 Sample Geometry and Specimen Holder

Samples for examination using off-axis electron holography must satisfy stringent geometrical requirements. There must be a vacuum region close to the area of interest and the sample thickness

must be close to the optimised membrane thickness for the material under examination (Rau et al 2002), which is usually ~ 200-300 nm for silicon. These requirements can be satisfied by FIB-prepared samples. However, a standard trench prepared FIB membrane is restricted in tilt to only ~ ± 10º due to shadowing by the trench walls, therefore making it unsuitable for tomography. A modified sample geometry has been prepared, illustrated in Fig. 1a, where a thin membrane is milled along the edge of a cleaved square of silicon that can be tilted through 360º without shadowing by the bulk specimen. This specimen was mounted in a Fischione two-contact electrical biasing tomography holder, illustrated in Fig. 1b, which is capable of tilts of ± 80º in the electron microscope. A silicon *p-n* junction device with nominal dopant concentrations of in excess of 10^{18}cm^{-3} in both *p* and *n* regions was prepared in this sample geometry for combined holography and tomography experiments.

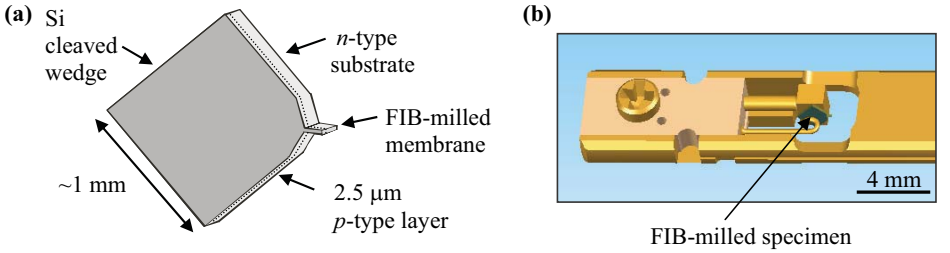

Fig. 1: (a) Schematic diagram of the sample geometry used for combined electron holography and tomography of a silicon *p-n* junction. (b) Diagram of the end of the Fischione TEM holder used for electrically biased electron tomography and holography.

2.2 Experimental Procedure

Off-axis electron holograms were acquired on a Philips CM300 field-emission TEM, which was operated in Lorentz mode and equipped with a Gatan imaging filter (GIF) 2000, using a biprism voltage of 100 V. Holograms were acquired over a tilt range of -70° to +70° at 2° intervals. Reference holograms were acquired every 10° in tilt in order to remove distortions associated with the imaging and recording system. Holograms were reconstructed immediately after acquisition using scripts written using Digital Micrograph software to ensure that the *p-n* junction was positioned within the field of view, as no alignment features on the sample are visible in an unprocessed hologram. Figure 2a shows an off-axis electron hologram acquired at zero degrees tilt (defined as the tilt that results in the junction being edge-on) and Fig. 2b shows the corresponding reconstructed phase image. Convergent beam electron diffraction was used to determine the crystalline thickness of the FIB-prepared membrane. This thickness was determined to be 330 nm, giving a total membrane thickness of 380 nm including the thickness of amorphous surface layers generated by FIB milling.

2.3 Data Analysis

Off-axis image and reference holograms were reconstructed to obtain phase and amplitude images using library programs written in the Semper image processing language (Saxton et al. 1979). The amplitude images were used to calculate normalised thickness (t/λ) maps of the specimen for each tilt angle. Figure 2c shows the t/λ map corresponding to the hologram in Fig. 2a, and Fig. 2d plots the variation in t/λ over the entire tilt range showing that a number of points lie away from the line of expected thickness variation. This variation may indicate that the specimen is in a strongly diffracting condition, which affects the measured phase and amplitude images, complicating the interpretation of the observed phase image. Such images were therefore excluded from the tomographic dataset used for 3-D reconstruction. At the specimen edge, a number of 2π phase 'wraps' are often present due to the abrupt thickness change present at the edge of the FIB-prepared specimen. These 'wraps' can lie directly on top of one another, preventing accurate phase unwrapping. In order to overcome this issue, the expected phase change was calculated (from the mean inner potential and thickness measurements) and used to determine the number of 2π wraps

present at the edge region. The phase in the specimen region in each reconstructed image was then adjusted to the corrected value.

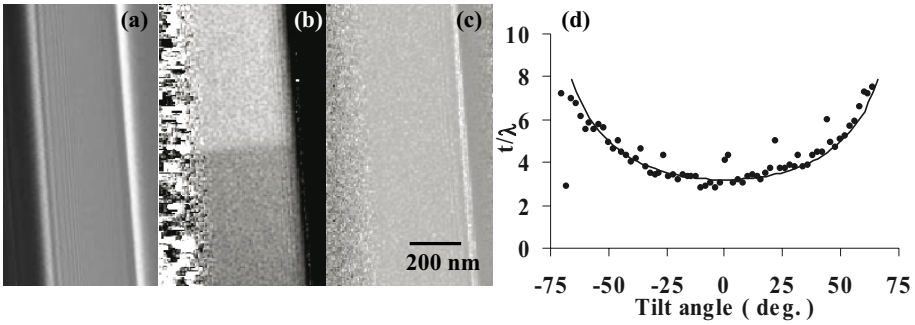

Fig. 2: (a) Off-axis electron hologram, (b) corresponding reconstructed phase image and (c) thickness (t/λ) map acquired at 0° tilt of the FIB-prepared silicon *p-n* junction. (d) Plot of the variation in thickness (t/λ) as a function of tilt angle. The solid line indicates the expected variation in thickness with tilt angle. The points lying away from the line indicate that the image is significantly affected by diffraction contrast. The corresponding images are excluded from the tomographic reconstruction.

From Fig. 2a, it can be seen that the original holograms do not contain any distinguishable features other than the interface between the specimen and the vacuum. The images were aligned using the interface to obtain a rotational and horizontal alignment, and using the junction position to align the images in the vertical direction. The simultaneous iterative reconstruction technique (SIRT) was used to reconstruct the 3-D electrostatic potential in the specimen. The thickness was constrained in the reconstruction to 380 nm (from the t/λ and CBED measurements) because the featureless membrane surfaces cannot be reconstructed accurately with the restricted tilt range due to the 'missing wedge' of information.

3. RESULTS AND DISCUSSION

A schematic diagram showing the expected electrostatic potential variation is shown in Fig. 3a, illustrating the amorphous and crystalline electrically inactive surface layers deduced previously (Twitchett et al 2004). The experimentally determined 3-D reconstructed electrostatic potential of the *p-n* junction, which is shown in Fig. 3b, can be observed qualitatively to show a comparable potential distribution to the expected variation. The voxel size in the reconstruction is 5.8 nm and the spatial resolution is 10 nm based on the Crowther equation (Crowther et al 1970). The phase resolution is 0.1 rad. (Lichte 1991). This 3-D data set can be used to extract information about the specimen, including line profiles across the *p-n* junction close to the centre and at the surfaces of the specimen. The tomographic reconstruction software re-scales the phase data automatically, and therefore the extracted experimental profiles have been adjusted such that the central profile (extracted from the 3-D dataset with a width of one voxel) matches the expected phase variation for bulk silicon. The potential variation indicated in Fig. 3b is only the dopant-related electrostatic potential, although the absolute value of the potential (relative to vacuum) can be used to determine the value of the mean inner potential (V_0). Theoretical line profiles, taken from simulations described elsewhere (Somodi et al 2003) are shown in Fig. 2c. Corresponding experimental line profiles are shown in Fig. 2d. These line profiles show good correlation between simulations and experimental results, indicating a significant increase in depletion width and a reduction in potential variation across the junction close to the membrane surfaces, due in part to the damage caused by FIB milling. Further simulations are required to model the point defects and amorphous layers present to provide a fully quantitative understanding of the potential at FIB-prepared sample surfaces. However, this preliminary result indicates that the near-surface layers of thin FIB-prepared membranes can make up a significant fraction of a TEM specimen, and must be considered carefully to provide a quantitative understanding of dopant potentials in semiconductor devices.

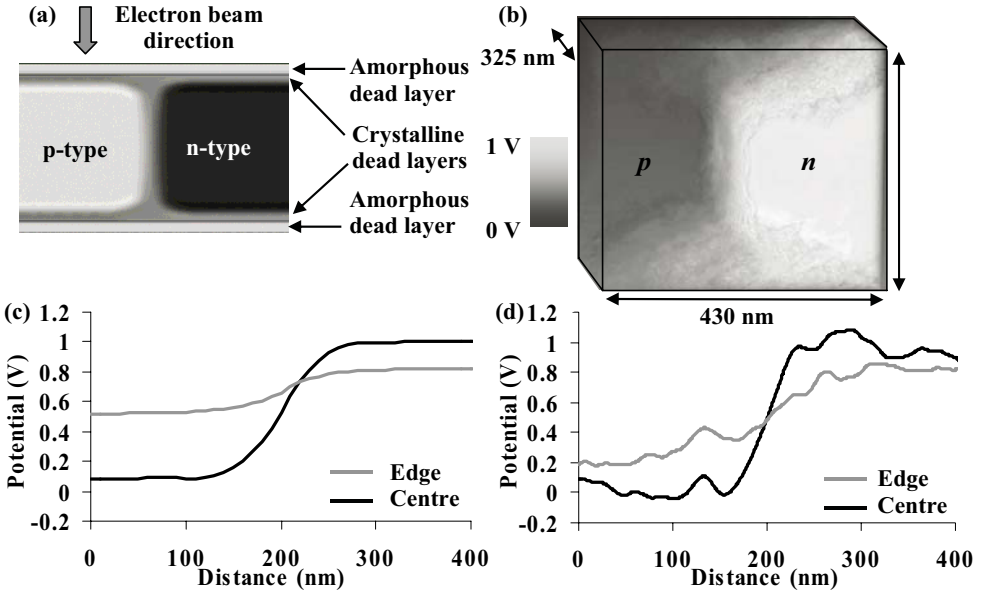

Fig. 3: (a) Schematic diagram showing the expected electrostatic potential variation in an FIB-prepared membrane containing a *p-n* junction. (b) Corresponding experimental 3-D electrostatic potential obtained using electron tomography. (c) Line profiles from the simulation of the expected electrostatic potential. (d) Experimental line profiles extracted from the centre and the edge of the tomographic reconstruction, showing the variation in electrostatic potential across the *p-n* junction.

4. CONCLUSIONS

Off-axis electron holography and tomography have been combined successfully to reconstruct the 3-D potential in a silicon FIB-prepared *p-n* junction device. The 3-D reconstruction provides information about the mean inner potential and dopant-related potential at any position in a thin specimen. Further work is required to optimise the tomographic reconstruction procedure to ensure a fully quantitative 3-D potential. This information could also be combined with an iterative reconstruction approach to use *ab initio* simulations to deduce the structures of the surface layers. Holographic tomography is a very promising technique for the quantitative examination of the 3-D electrostatic potential in semiconductor devices.

ACKNOWLEDGEMENTS

The authors would like to thank Dr R F Broom for his assistance and advice, Philips Research Laboratories (Eindhoven) for providing the silicon device and Newnham College, the Royal Society and the EPSRC for financial support.

REFERENCES

Crowther T A, DeRosier D J and Klug A 1970 Proc Roy Soc Lond **A317**, 319

Lichte H 1991 Ultramicroscopy **38**, 13

McCartney M R, Gribelyuk M A, Li J, Ronsheim P, McMurray J S and Smith D J 2002 Appl Phys Lett **80**, 3213

Midgley P A and Weyland M 2003 Ultramicroscopy **96**, 413

Rau W D, Schwander P, Baumann F H, Hoppner W and Ourmazd A 1999 Phys Rev Lett **82**, 2614

Somodi P K, Dunin-Borkowski R E, Twitchett A C, Barnes C H W and Midgley P A 2003 Inst Phys Conf Ser **180**, 501

Twitchett A C, Dunin-Borkowski R E, Hallifax R J, Broom R F and Midgley P A 2005 Microsc. Microanal. **11**, 66